

Robust Directional-Diffusive Hybrid Molecular Communication with Parity-check Erasure Coding

Hiroaki Egashira^{*‡}, Junichi Suzuki^{*}, Jonathan S. Mitzman^{*}, Tadashi Nakano[†] and Hiroaki Fukuda[‡]

^{*}University of Massachusetts, Boston

Department of Computer Science

Boston, MA 02125, USA

Email: {hiroaki, jxs, tolkien}@cs.umb.edu

[†]Osaka University

Graduate School of Frontier Biosciences and Institute for Academic Initiatives

Osaka 565-0871, Japan

Email: tadasi.nakano@fbs.osaka-u.ac.jp

[‡]Shibaura Institute of Technology

Department of Information Science and Engineering

Tokyo 135-8548, Japan

Email: hiroaki@shibaura-it.ac.jp

Abstract—This paper investigates a robustness enhancement protocols for biologically-enabled machines (or bio-nanomachines) to reliably exchange information by means of molecules in the aqueous, intrabody environment. The proposed protocol performs forward error correction (FEC) for directional-diffusive hybrid transports, in which molecules travel through two different transports: directional and diffusive transports. It allows the transmitter bio-nanomachine to encode molecules in a redundant manner with parity-check erasure codes. The receiver bio-nanomachine can recover the information embedded in lost molecules. Simulation results show that the proposed protocol enhances robustness against molecule losses and in turn improves communication performance. They also reveal the impacts of FEC overhead and molecule redundancy on the communication performance.

I. INTRODUCTION

Molecular communication is an emerging paradigm to network biologically-enabled machines (or *bio-nanomachines*) in the intrabody environment [1]–[5]. Bio-nanomachines are nano-to-micro scale devices that exchange information by means of molecules and perform simple computation, sensing and/or actuation tasks. Molecular communication is expected to enable various biomedical and healthcare applications such as nanoscale lab-on-a-chip, in-situ physiological sensing, targeted drug delivery, artificial morphogenesis and neural signal transduction [2], [3], [6], [7].

This paper considers molecular communication where bio-nanomachines transmit and receive information-encoded molecules (or *information molecules*) in aqueous environments. It is known inherently unreliable due to stochastic molecular propagation, molecule-to-molecule collisions and environmental noise. They cause extremely long latency, large jitter, high molecule loss rate and low capacity in [8], [9].

In order to address this reliability issue, this paper proposes a robustness enhancement protocol for *directional-diffusive hybrid transports*, in which information molecules travel through two different transports: (1) *directional transport* where information molecules directionally move on pre-defined protein filaments (e.g., microtubules or actin filaments) by using molecular motors such as kinesin, dynein and myosin, and (2) *diffusive transport* where information molecules propagate subject solely to the laws of diffusion. The proposed protocol allows the transmitter bio-nanomachine (Tx) to perform forward error correction (FEC) with parity-check erasure coding. The Tx produces parity-check codes from given information molecules and propagate the codes along with the molecules. The receiver bio-nanomachine (Rx) can recover the information embedded in lost molecules by taking advantage of the parity-check codes. Simulation results demonstrate that the proposed protocol enhances robustness against molecule losses and in turn improves communication performance such as latency and jitter. When a single information molecule is transmitted for 90 μm in between the Tx and Rx, the proposed protocol improves latency by 15% and latency jitter by 80% with the FEC overhead (code rate) of 50%. The improvements in latency and jitter become 21 % and 64 %, respectively, by duplicating the information molecule 100 times.

II. BACKGROUND AND RELATED WORK

Applications of molecular communication have been considered in various domains [3], [6]. This section briefly summarizes a few biomedical and healthcare applications.

Lab-on-a-chip: Chemical analysis of biological samples is performed on a chip with dimensions in the millimeter to centimeter range for diagnosis of diseases and other scientific purposes. Molecular communication provides a means to transport specific molecules from sensory components (e.g., biosensors) in a chip to other components in the chip (e.g.,

chemical reactors). In a potential implementation, a sensory component binds specific molecules in a sample to a certain “interface” molecule or places the molecules in an organelle. A molecular motor carries the interface molecule or organelle and moves on a microtubule from a sensory component to a chemical reactor component [10]. Molecular communication may have advantages because it uses molecular-level mechanisms for directly manipulating the molecules in a sample and does not require translation of information to/from electrical signals. In addition, molecular communication may allow lab-on-a-chip applications to scale further down since molecular communication components can be at the nanometer scale.

Physiological monitoring: A specific type of molecules can serve as a bio-marker for a disease or a certain physiological condition in the body. Implanted bio-nanomachines may exploit sensory components (e.g., biosensors) to detect specific molecules, gather/aggregate information about the detected molecules (e.g., concentration and spatial distribution of molecules) and utilize molecular communication as a means of delivering the information to subdermal devices, which in turn communicate to on-body external devices [6], [11].

In the area of molecular communication, major research efforts have focused on the physical layer’s characteristics such as channel capacity, latency, signal attenuation and energy requirements (e.g., [8]–[10], [12], [13]). This paper sits on these existing work to investigate a higher-layer issue: reliable molecular transmission via robustness enhancement against molecule losses.

There exist several relevant work to enhance the reliability of short-range molecular communication in aqueous environments [14]–[18]. Nakano et al. [15] and Felicetti et al. [16] study feedback-based rate control schemes for diffusive molecule propagation. Those schemes are designed to ensure delivering a given number of information molecules to the receiver bio-nanomachine (Rx) while preventing the transmitter bio-nanomachine (Tx) from transmitting molecules faster than the Rx reacts. Nakano et al. examine both positive and negative feedback schemes [15], and Felicetti et al. examine a negative feedback scheme [16].

While in-sequence delivery of information molecules is out of the scope of [15], [16], Wang et al. [17], Bai et al. [18] and Mitzman et al. [14] study in-sequence and at-least-once delivery schemes with positive feedbacks. The Rx is designed to explicitly acknowledge information molecules and request the Tx to retransmit lost ones based on Stop-and-Wait Automatic Repeat Request (SW-ARQ) [19]. (Implicit acknowledgement is used in [15], [16].) Diffusive molecular transports are considered in [17] and [18]. Mitzman et al. consider diffusive, directional and diffusive-directional hybrid transports [14].

This paper approaches reliability in molecule transmission with forward error correction (FEC) instead of feedback-based schemes, which require bi-directional channels between the Tx and the Rx. In this paper, erasure coding allows the Rx to recover lost information molecules without requesting the Tx to retransmit them. Only a forward channel is assumed from

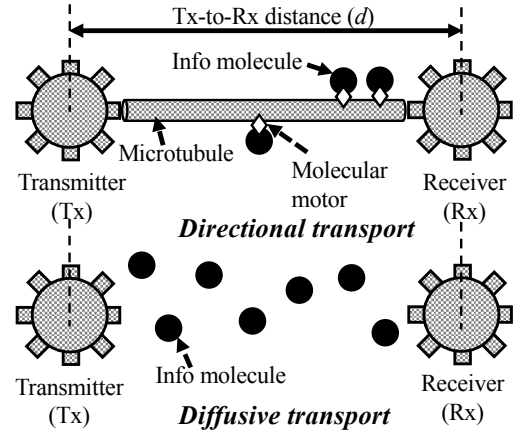


Fig. 1. Directional and Diffusive Transports

the Tx to the Rx by eliminating the Rx-to-Tx reverse channel at the cost of a fixed, higher forward channel bandwidth. This paper is similar to [18], [20]–[25] in that those papers utilize FEC. Hamming codes, cyclic redundancy check (CRC) codes, self-orthogonal convolutional codes (SOCCs) and minimum energy codes (MECs) are used for the Rx to detect and correct bit errors in information molecules in [18], [20]–[25], respectively. Recovery of lost molecules is out of their scope.

Furubayashi et al. propose packet fragmentation and reassembly in molecular communication [26]. This paper shares the same assumptions for packetized molecular communication with [26]. It complements the findings in [26], which are obtained through numerical analysis with a one-dimensional, collision-free environment, by simulating three-dimensional molecular diffusion in a collisional environment where collisions occur among molecules. Although Furubayashi et al. consider packet reassembly at the Rx, recovery of lost molecules (i.e., lost packets) is out of their scope.

III. THE PROPOSED ROBUSTNESS ENHANCEMENT PROTOCOL

This section describes the proposed protocol.

A. Directional-Diffusive Hybrid Communication Model

This paper assumes a bounded three-dimensional aqueous environment in which the transmitter bio-nanomachine (Tx) and the receiver bio-nanomachine (Rx) exchange information molecules that carry certain messages (information) (Fig. 1). The Tx releases information molecules with an active transport, which utilizes a microtubule in between the Tx and the Rx. Based on some findings in biomedical engineering (e.g., [27]), the microtubule is configured to directionally guide molecular motors (e.g., kinesin, dynein and myosin) from one end (Tx) to the other end (Rx). Information molecules are attached to molecular motors, and they travel toward the Rx as the molecular motors move along the microtubule. In this paper, a microtubule is assumed to be stiff, straight and fixed-length cylinder.

On a microtubule, a molecular motor moves at a constant velocity for an expected length (distance walking along a microtubule before randomly moving away). It also moves away when it collides with molecules or other molecular motors on a microtubule. Once detached from a microtubule, an information molecule with a molecular motor performs a pure random walk through a diffusive transport (Fig. 1). Diffusive movement is governed by the diffusion coefficient D on each dimension: $D = \partial x^2 / (2 \times \partial t)$ independently in three dimensions. x denotes the distance of molecular movement during an amount of time t . When an information molecule collides with another molecule, it randomly moves to another position with D . While diffusing, an information molecule may contact a microtubule and begin to walk along the microtubule. The Rx is assumed to capture an information molecule when it has a physical contact with the molecule.

Given wet laboratory implementations of molecular communication (e.g., [28]), this paper assumes DNA molecules as information molecules that can contain messages by means of nucleotide sequences. DNA is structurally defined as a linear chain of repeating units of deoxyribonucleotide. Each deoxyribonucleotide is composed of a nucleobase, either adenine (A), guanine (G), cytosine (C) or thymine (T), as well as a five-carbon sugar called deoxyribose, and a phosphate group. A nucleobase of DNA encodes 2 bits of information because there are four choices (A, G, C and T), and it has a length of approximately 0.34 nm per nucleobase [2]; thus, up to 5,882 bits/ μm can be achieved. Molecular communication with large (heavy) molecules like DNA molecules have advantages over conventional molecular communication with small (lightweight) molecules (e.g., [8], [9]) in that large molecules can carry high-density information.

Promising approaches to engineer bio-nanomachines with communication capability include the modification of biological cells and the production of artificial cell-like structures using biological materials (e.g., a vesicle embedded with proteins) [13]. This paper assumes that bio-nanomachines are realized as modified biological cells, which are known to potentially possess various communication-related functions including a transmission function to synthesize and release specific molecules, a reception function to capture molecules, logic gates to trigger programmed chemical responses upon receiving molecules, toggle switches (i.e., 1-bit memories) to retain communication-related states (e.g., ready-to-transmit and in-transmission/waiting states), and oscillators (i.e., clocks) to control the temporal timing of releasing molecules.

B. Packetization of Information Molecules

The proposed protocol employs the notion of packet fragmentation and reassembly [26]. As Fig. 2 shows, the Tx *packetizes* a large information molecule (i.e., a large DNA molecule containing a long nucleobase chain) into smaller pieces (i.e., smaller DNA molecules containing shorter nucleobase chains) and propagate the packetized information molecules in the environment. The Rx receives these packetized information molecules (or *molecular packets*) and reassembles the original

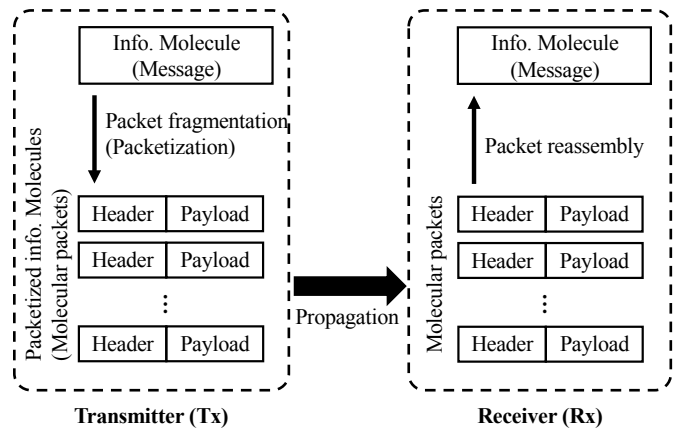


Fig. 2. Packet Fragmentation and Reassembly

information molecule. Packetization of information molecules is motivated by the findings that, compared to larger ones, smaller DNA molecules diffuse faster [29] and arrive at the Rx with higher probability [26].

Each molecular packet is assumed to be uniquely identifiable. It consists of a payload and a header (Fig. 2). A payload contains a fragment of the original message. A header contains control information such as a receiver address to which the molecular packet is delivered, an identifier (or sequence number) for the original message that the molecular packet belongs to, and an identifier for the molecular packet.

The packet fragmentation and reassembly may be implemented by exploiting enzymes from biological cells, e.g., restriction enzymes to cut a DNA molecule into smaller fragments, and DNA ligases to join two DNA fragments into a larger one. Restriction enzymes may be embedded in the Tx and DNA ligases in the Rx. Chemical reactions to implement the packet fragmentation and reassembly are simple and require these enzymes and a few small cofactors. The biochemical reaction to cut a DNA molecule into fragments is a hydrolysis reaction, which requires no energy. On the other hand, the biochemical reaction to concatenate DNA molecules requires chemical energy. The energy cost required for the proposed molecular communication scheme increases linearly with respect to the number of fragments.

C. Parity-check Erasure Coding

The proposed protocol leverages parity-check erasure coding as a forward error correction mechanism. The Tx applies exclusive-or (XOR) operations to a group of m molecular packets to obtain k fixed-length *parity codes* and generates extra k packets, called *parity packets*, which contain the parity codes. The Tx propagates $m + k$ packets to the environment. The Rx can tolerate up to k packet losses. It can recover the original m molecular packets with $(m - k)$ packets. Packet code rate (PCR) is denoted as k/m .

Fig. 3 illustrates a simple example where $m = 10$ and $k = 1$ (PCR = 10%). The Tx propagates 11 packets in total: 10 molecular packets and one parity packet that contains bitwise

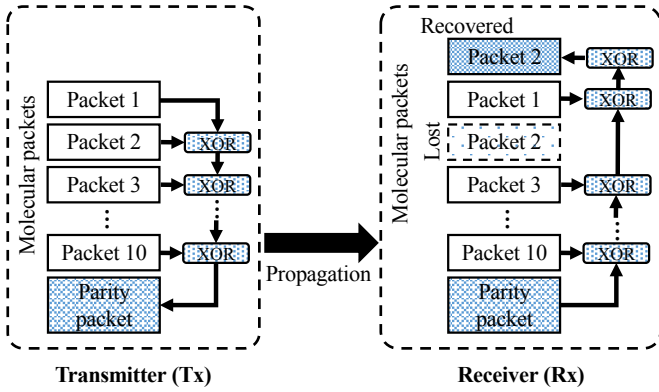


Fig. 3. Parity-check Erasure Coding

XOR on the 10 molecular packets as parity code. The Rx can recover one lost packet (Packet 2 in Fig. 3) with nine molecular packets and one parity packet. In order to increase PCR, the number of molecular packets is decreased to produce parity code. For example, in Fig. 3, two parity packets can be generated by producing parity code from five molecular packets (PCR = 20%). five parity packets can be generated by producing parity code from two packets (PCR = 50%).

IV. SIMULATION EVALUATION

This section evaluates the proposed robustness enhancement protocol through simulations. Table I shows simulation parameter settings, which follow findings in biomedical engineering (e.g., [27], [29]). Every result is shown based on 1,000 independent simulations.

TABLE I
PARAMETER SETTINGS

Parameter	Value
Size of the environment	150 μm x 150 μm x 150 μm
Diameter of Tx and Rx	5 μm
Tx to Rx distance (d)	30, 50, 70 and 90 μm
Length of an info. molecule (L_m)	10.2 μm
Degree of packetization (n)	1, 10 and 100
Diffusion coefficient of a mol. packet (D)	0.70, 2.73 and 9.84
Velocity of a molecular motor on a microtubule	1 $\mu\text{m/s}$
Expected travel distance of a molecular motor on a microtubule	4 μm
Diameter of a molecular packet ($R \times 2$)	0.98, 0.25 and 0.07 μm
Parity code rate (PCR)	0, 10, 20 and 50 %
# of duplications of an info. molecule	1, 10 and 100

This paper simulates a DNA molecule, as an information molecule, which contains a 10.2 μm long nucleobase chain (L_m). It is assumed to have 30,000 nucleobase pairs [29] and encode a message of 60,000 bits. The length of each molecular packet (L_p) is calculated as follows:

$$L_p = L_m/n + L_h \quad (1)$$

n denotes the number of divisions on an information molecule (i.e., the number of packets generated from the information molecule). L_m/n indicates the length of a payload

(Fig. 2). L_h denotes the length of a header. 60 nucleobase pairs (120 bits) are allocated for a header in this paper ($L_h = 0.0204 \mu\text{m}$).

The diffusion coefficient D and the radius R of a molecular packet are derived from the following equations [29].

$$D = \alpha L_p^{-\beta} \quad (2)$$

$$R = \gamma/D \quad (3)$$

Experimentally obtained values are used for α , β and γ [29]: $\alpha = 2.8$, $\beta = 0.6$ and $\gamma = 3.4$.

Figs. 4 and 5 show how Tx-to-Rx distance (d), parity code rate (PCR) and packetization degree (n , i.e., the number of molecular packets) impact communication latency of a single information molecule to arrive at the Rx. When $n = 1$, an information molecule is not packetized. It appends a header to its payload (message) and travels to the Rx. When $n > 1$, an information molecule is packetized. Each packet appends a header its payload and travels to the Rx (Fig. 2). When PCR = 0, erasure coding is not performed. In this paper, latency indicates the interval between the time when a packet leaves the Tx and the time when the Rx reassembles a transmitted message by receiving a necessary set of packets.

Figs. 4 and 5 illustrate that both median and average latency improve as PCR increases. When the degree of packetization is 10 ($n = 10$), average latency decreases by 45% as PCR increases from 0 to 50% ($d = 90 \mu\text{m}$). When $n = 100$, it decreases by 46% as PCR increases from 0 to 50% ($d = 90 \mu\text{m}$). These results demonstrate that the proposed protocol is robust against packet losses and improves latency performance.

Compared to the case where an information molecule is transmitted with packetization disabled ($n = 1$ and PCR = 0), the proposed protocol decreases average latency by 18% and 15% when the degree of packetization is 10 and 100, respectively ($d = 90$ and PCR = 50%). The proposed protocol successfully takes advantage of packetization and erasure coding to make improvements in latency performance.

Fig. 6 depicts the average number of collisions in a single simulation. This paper assumes that all molecular packets collide with each other. The number of collisions grows as the degree of packetization (n) increases. However, it is very low even when $n = 100$. 100 molecular packets collide less than 5 times on average in a single simulation ($n = 100$, $d = 90 \mu\text{m}$ and PCR = 50%).

Figs. 7 and 8 show how Tx-to-Rx distance (d), parity code rate (PCR) and packetization degree (n) impact latency in transmitting 10 duplicated information molecules. Figs. 10 and 11 show the latency of transmitting 100 duplicated information molecules. All duplicated molecules contain the same message. When packetization is enabled ($n > 1$), each of the duplicated molecules is fragmented to packets. Latency indicates the interval between the time when packets leave the Tx and the time when the Rx reassembles at least one message.

Figs. 4, 5, 7, 8, 10 and 11 illustrate that duplication of molecules aids improving latency. The shortest average latency

(3,228 seconds) is recorded when 100 duplicated information molecules are transmitted with $n = 100$, PCR = 50% and $d = 90 \mu\text{m}$ (Fig. 11). It is 21 % lower than the latency of transmitting 100 duplicated information molecules with packetization disabled (4109 seconds).

Fig. 8 shows that the proposed protocol improves latency by 44% as it increases PCR from 0% to 50% when 10 duplicated information molecules are used ($n = 100$ and $d = 90 \mu\text{m}$). Fig. 11 shows that the proposed protocol improves latency by 34% as it increases PCR from 0% to 50% when 100 duplicated molecules are used ($n = 100$ and $d = 90 \mu\text{m}$). Similar to an observation in Figs. 5, Figs. 8 and 11 demonstrate that the proposed protocol is robust against packet losses and improves latency performance via packetization and erasure coding.

Another finding from Figs. 5, 8 and 11 is that the impacts of PCR on latency decreases as the number of duplicated molecules increases. Latency improvement due to the 0% to 50% increase of PCR decreases from 46% to 34% as the number of duplicated molecules grows from 1 to 100. This is caused by the increase in the number of collisions among molecular packets (Figs. 6, 9 and 12). Molecular packets collide with each other more than 3,000 times in a single simulation when 100 duplicated information molecules are used (Fig 12). In contrast, the number of collisions is less than five when a single information molecule is used (Fig. 6). Higher occurrence of collisions also makes latency performance comparable between the two cases: the case where no packetization is performed ($n = 1$ and PCR = 0) and the case where packets are generated but erasure coding is not performed ($n > 1$ and PCR = 0) (Fig. 11).

Table II shows how latency jitter changes under different simulation settings. Jitter is computed as a standard deviation of latency results in 1,000 independent simulations. As illustrated in Table II, the proposed protocol yields lower jitter as the degree of packetization (n) and PCR increase. With a single information molecule, jitter decreases by 80% as n increases from 0 to 100 and PCR increases from 0 to 50% ($d = 90\mu\text{m}$). With 10 and 100 duplicated molecules, jitter decreases by 62% and 64%, respectively, as n increases from 0 to 10 and PCR increases from 0 to 50% ($d = 90\mu\text{m}$). Table II demonstrates that the proposed protocol successfully leverages packetization and erasure coding to substantially decrease latency jitter and make latency performance more predictable.

V. CONCLUSION

This paper investigates a protocol designed to enhance robustness of molecular communication against molecule losses. Simulation results demonstrate that the proposed protocol is robust against molecule losses and in turn improves communication performance such as latency and jitter. When communication distance is $90 \mu\text{m}$ between the Tx and the Rx, the proposed protocol improves latency by 15% and latency jitter by 80% through fragmenting an information molecule to 100 packets with the parity code rate (PCR) of 50%. The improvements in latency and jitter are 21 % and 64

%, respectively, when fragmenting each of 100 duplicated information molecules to 100 packets with 50 % PCR.

REFERENCES

- [1] T. Suda, M. Moore, T. Nakano, R. Egashira, and A. Enomoto, "Exploratory research on molecular communication between nanomachines," in *Proc. ACM Genetic and Evol. Computat. Conference*, 2005.
- [2] T. Nakano, A. Eckford, and T. Haraguchi, *Molecular Communication*. Cambridge University Press, 2013.
- [3] I. Akyildiz, F. Brunetti, and C. Blazquez, "Nanonetworks: a new communication paradigm," *Comput. Netw.*, vol. 52, 2008.
- [4] A. Goel and V. Vogel, "Harnessing biological motors to engineer systems for nanoscale transport and assembly," *Nat. Nanotechnol.*, vol. 3, pp. 465–475, 2008.
- [5] P. E. M. Purnick and R. Weiss, "The second wave of synthetic biology from modules to systems," *Nat. Rev. Mol. Cell Bio.*, vol. 10, no. 6, pp. 410–422, 2009.
- [6] Y. Moritani, S. Hiyama, and T. Suda, "Molecular communication for health care applications," in *IEEE Int'l Conf. Pervasive Comput. Commun. Workshops*, 2006.
- [7] J. Suzuki, D. H. Phan, and H. Budiman, "A nonparametric stochastic optimizer for TDMA-based neuronal signaling," *IEEE Trans. NanoBioscience*, vol. 13, no. 3, pp. 244–254, 2014.
- [8] M. Pierobon and I. F. Akyildiz, "Diffusion-based noise analysis for molecular communication in nanonetworks," *IEEE Trans. Signal Process.*, vol. 59, no. 6, 2011.
- [9] K. V. Srinivas, R. S. Adve, and A. W. Eckford, "Molecular communication in fluid media: The additive inverse gaussian noise channel," *IEEE Trans. Inf. Theory*, vol. 58, no. 7, 2012.
- [10] N. Farsad, A. Eckford, S. Hiyama, and Y. Moritani, "A simple mathematical model for information rate of active transport molecular communication," in *IEEE INFOCOM Wksp Mol Nanosc Comm*, 2011.
- [11] R. A. Freitas, "Current status of nanomedicine and medical nanorobotics," *J. Computational and Theoretical Nanoscience*, vol. 2, no. 1, pp. 1–25, 2005.
- [12] M. J. Moore and T. Suda, "Molecular communication: Modeling noise effects on information rate," *IEEE Trans. NanoBiosci.*, vol. 8, no. 2, 2009.
- [13] T. Nakano, M. Moore, F. Wei, A. V. Vasilakos, and J. W. Shuai, "Molecular communication and networking: opportunities and challenges," *IEEE Trans. NanoBiosci.*, vol. 11, no. 2, pp. 135–148, 2012.
- [14] J. S. Mitzman, B. Morgan, T. M. Soro, J. Suzuki, and T. Nakano, "A feedback-based molecular communication protocol for noisy intrabody environments," in *17th IEEE Int'l Conference on E-health Networking Applications and Services*, 2015.
- [15] T. Nakano, Y. Okaie, and A. V. Vasilakos, "Transmission rate control for molecular communication among biological nanomachines," *IEEE J. Sel. Area Comm.*, vol. 31, no. 12, pp. 835–846, 2013.
- [16] L. Felicetti, M. Femminella, G. Reali, T. Nakano, and A. V. Vasilakos, "TCP-like molecular communications," *IEEE J. Sel. Area Comm.*, vol. 32, no. 12, pp. 2354–2367, 2014.
- [17] X. Wang, M. D. Higgins, and M. S. Leeson, "Simulating the performance of SW-ARQ schemes within molecular communications," *Simulation Modelling Practice and Theory*, vol. 42, 2014.
- [18] C. Bai, M. S. Leeson, and M. D. Higgins, "Performance of SW-ARQ in bacterial quorum communications," *Nano Commun. Netw.*, vol. 6, no. 1, 2015.
- [19] H. O. Burton and D. D. Sullivan, "Errors and error control," *Proc. of the IEE*, vol. 60, no. 11, 1972.
- [20] M. S. Leeson and M. D. Higgins, "Forward error correction for molecular communications," *Nano Commun. Netw.*, vol. 3, no. 3, pp. 161–167, 2012.
- [21] —, "Error correction coding for molecular communications," in *2012 IEEE International Conference on Communications (ICC)*. IEEE, 2012, pp. 6172–6176.
- [22] Y. Lu, M. D. Higgins, and M. S. Leeson, "Self-orthogonal convolutional codes (socc) for diffusion-based molecular communication systems," in *2015 IEEE International Conference on Communications (ICC)*. IEEE, 2015, pp. 1049–1053.
- [23] C. Bai, M. S. Leeson, and M. D. Higgins, "Minimum energy channel codes for molecular communications," *Electronics Letters*, vol. 50, no. 23, pp. 1669–1671, 2014.

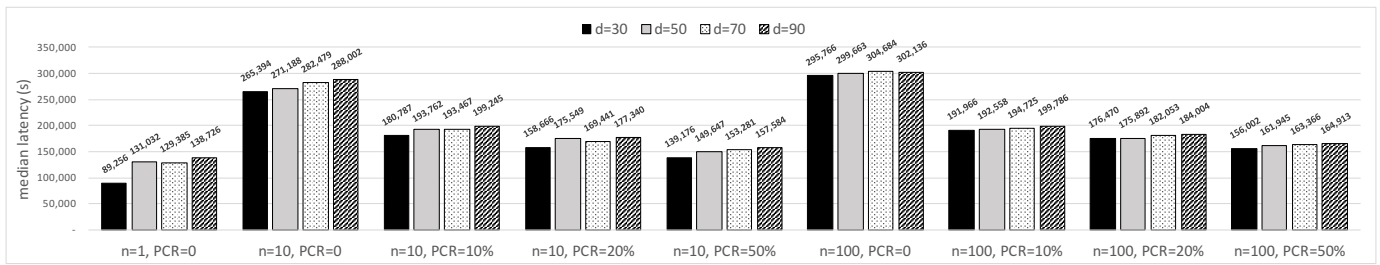


Fig. 4. Median Communication Latency with a Single Information Molecule

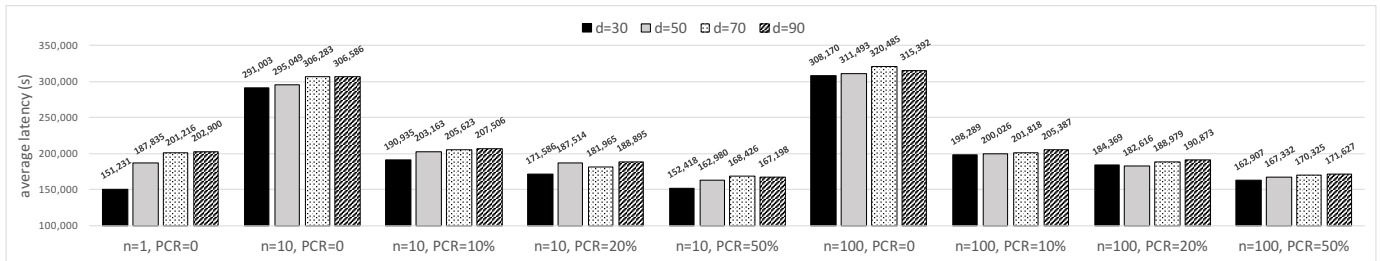


Fig. 5. Average Communication Latency with a Single Information Molecule

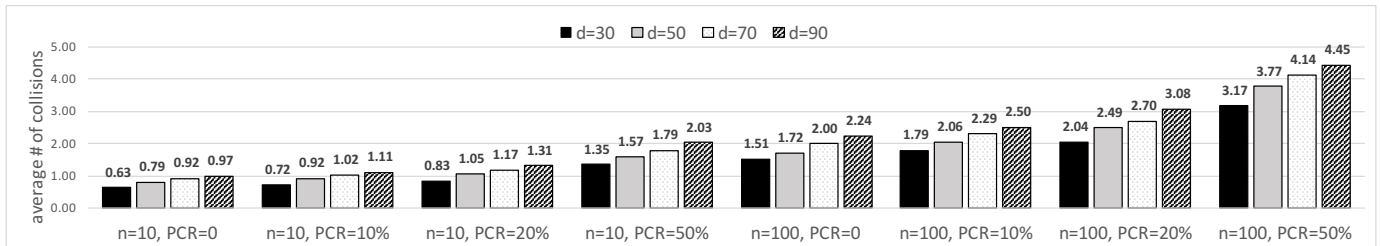


Fig. 6. Average Number of Collisions among Molecular Packets Fragmented from a Single Info. Molecule

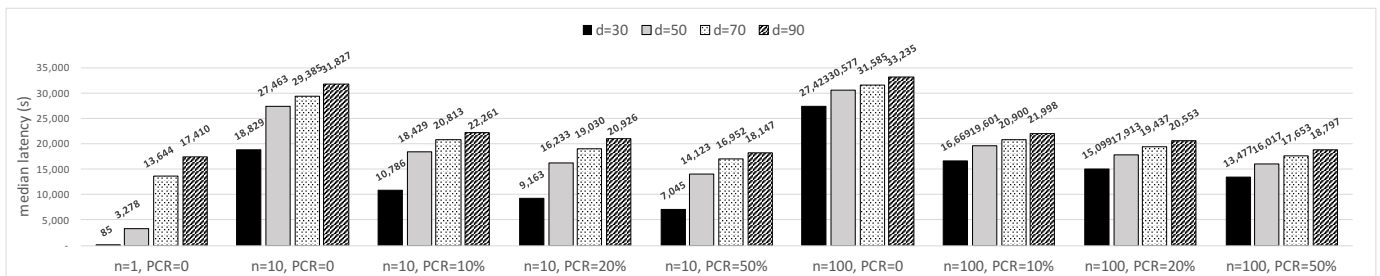


Fig. 7. Median Latency with 10 Information Molecules

- [24] Y. Lu, M. D. Higgins, and M. S. Leeson, "Comparison of channel coding schemes for molecular communications systems," *IEEE Transactions on Communications*, vol. 63, no. 11, pp. 3991–4001, 2015.
- [25] —, "Diffusion based molecular communications system enhancement using high order hamming codes," in *Communication Systems, Networks & Digital Signal Processing (CSNDSP), 2014 9th International Symposium on*. IEEE, 2014, pp. 438–442.
- [26] T. Furubayashi, T. Nakano, A. Eckford, Y. Okaie, and T. Yomo, "Packet fragmentation and reassembly in molecular communication," *IEEE Trans. NanoBiosci.*, vol. 15, no. 3, 2016.
- [27] R. D. Vale, T. Funatsu, D. W. Pierce, L. Romberg, Y. Harada, and T. Yanagida, "Direct observation of single kinesin molecules moving along microtubules," *Nature*, vol. 380, 1996.
- [28] M. E. Ortiz and D. Endy, "Engineered cell-cell communication via DNA messaging," *J. Biol. Eng.*, vol. 6, no. 16, 2012.
- [29] D. E. Smith, T. T. Perkins, and S. Chu, "Dynamical scaling of dna diffusion coefficients," *Macromolecules*, vol. 29, 1996.

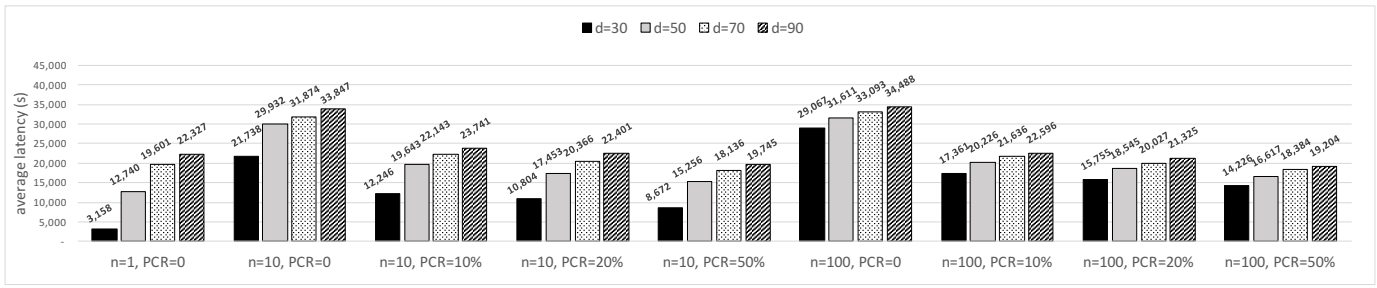


Fig. 8. Average Latency with 10 Information Molecules

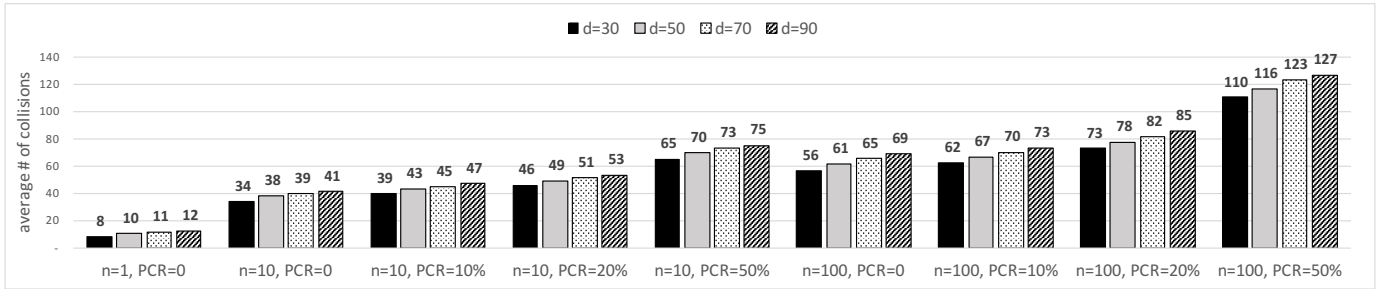


Fig. 9. Average Number of Collisions among Molecular Packets Fragmented from 10 Information Molecules

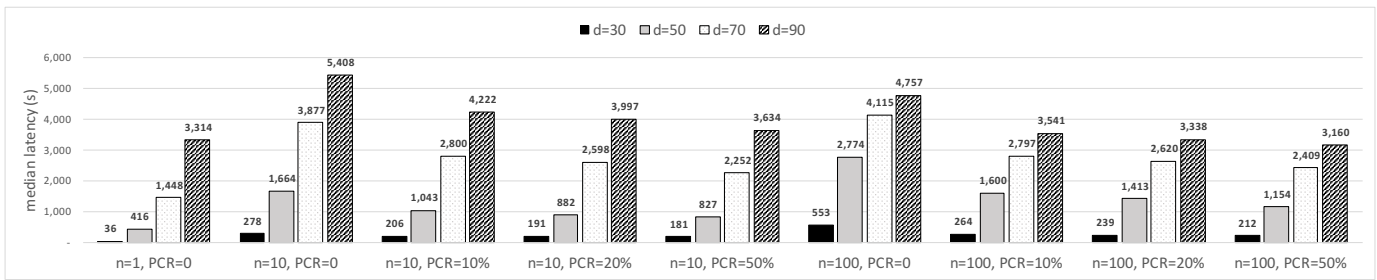


Fig. 10. Median Latency with 100 Information Molecules

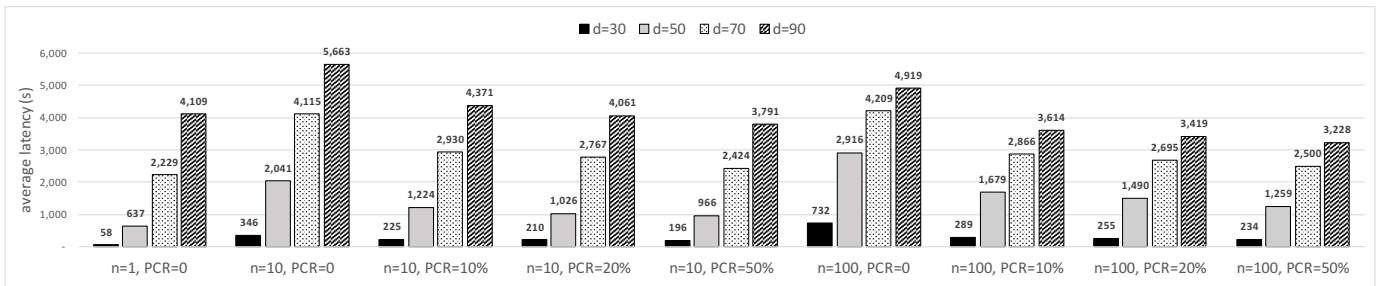


Fig. 11. Average Latency with 100 Information Molecules

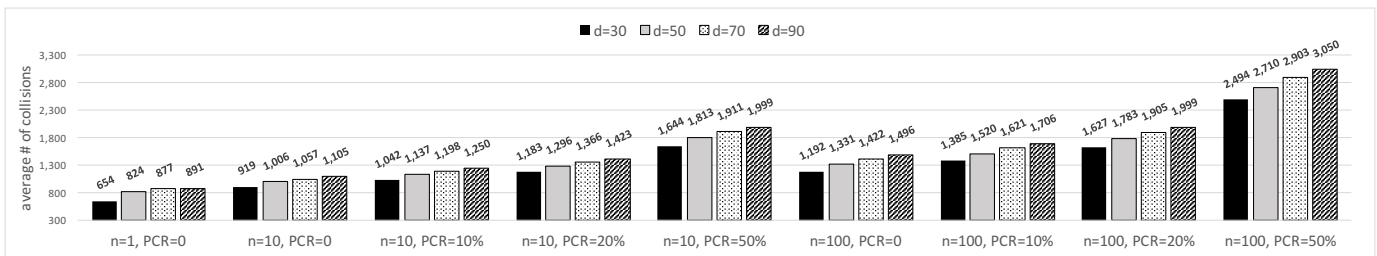


Fig. 12. Average Number of Collisions among Molecular Packets Fragmented from 100 Information Molecules

TABLE II
 JITTER (STANDARD DEVIATION) OF LATENCY PERFORMANCE

# of duplicated molecules	Comm. distance (d)	Degree of packetization (n)	PCR	STDEV of latency		
1	30 μm	1	0	178,055		
			10 %	78,291		
			20 %	72,300		
		10	50 %	69,276		
				10 %	42,632	
				20 %	43,611	
			100	39,133		
				187,520		
				10 %	74,562	
	50 μm	1	20 %	74,080		
			50 %	72,620		
			10 %	45,754		
		10	20 %	39,326		
				50 %	38,394	
				10 %	214,662	
			70 μm	1	10 %	77,518
					20 %	69,188
					50 %	72,964
	10	10 %		41,237		
				20 %	42,634	
				50 %	40,401	
		90 μm		1	0	203,100
					10 %	75,199
					20 %	72,145
10	50 %		65,001			
			10 %	40,143		
			20 %	40,003		
	100		40,758			
			9,802			
			10 %	8,326		
10	30 μm	1	20 %	8,043		
			50 %	6,980		
			10 %	4,392		
		10	20 %	4,201		
				50 %	4,139	
				18,052		
			50 μm	1	10 %	8,074
					20 %	7,439
					50 %	7,214
	10	10 %		4,057		
				20 %	4,208	
				50 %	3,865	
		70 μm		1	0	19,786
					10 %	8,096
					20 %	8,133
	10		50 %	7,241		
				10 %	4,474	
				20 %	4,324	
			90 μm	1	50 %	4,004
					19,676	
					10 %	7,926
	10	20 %		8,113		
				50 %	7,432	
				10 %	4,563	
100		4,543				
		4,196				
		54				
100	30 μm	1	10 %	87		
			20 %	75		
			50 %	66		
		10	10 %	111		
				20 %	71	
				50 %	104	
			50 μm	1	0	772
					10 %	666
					20 %	509
	10	50 %		505		
				10 %	492	
				20 %	472	
		100		442		
				2,364		
				10 %	1,018	
	70 μm	1	20 %	1,043		
			50 %	948		
			10 %	503		
		10	20 %	521		
				50 %	497	
				2,955		
			90 μm	1	10 %	1,138
					20 %	1,054
					50 %	1,056
10	10 %	515				
		20 %		481		
		50 %		496		